Automatic Crater Detection at the Lunar South Pole.

Ara V Nefian[1], Mark Shirley[2],Tony Colaprete[2], and Rick Elphic[2], [1]KBR, NASA Ames Research Center, MS 245-3, Moffett Field, CA, USA (ara.nefian@nasa.gov),[2]NASA

Age and size characterization of Lunar craters plays a significant role in Lunar science as well as in mission planing. The first step in achieving this goal is building of a large scale, high accuracy crater detection system. Current methods in crater detection include both manual and automatic methods. While manual crater detection is impractical given the large amount of data made available by Lunar orbital missions, the accuracy of the automatic methods is often limited by the crater size, and by varying illumination conditions. The proposed fully automatic method has been tested successfully in Lunar Pole LRO-NAC imagery for craters down to 8m in diameter and captured in various illumination conditions.

Introduction

Automatic crater detection methods [1], [2], [3], [4], use as input either images or digital elevation models (DEM). The methods that use DEMs benefit from illumination condition invariance but are limited to craters that are larger in size. This is due to the fact that current DEM products have lower resolution than the imagery. The method proposed in this paper uses both image and DEM information to detect craters fully automatically in various illumination conditions and at size that approaches the image ground resolution. The classification method, that uses neural networks, can also be used to detect craters when only images are available. However, in this case the model needs to be retrained for the specific illumination conditions.

Proposed Method

The proposed method trains a neural network using deep learning from manually labeled data (Figure 1). The labeled data consists of three classes: craters, flat regions with no craters and shadows. During training each pattern is scaled to 32×32 pixels. Both training and testing set consists of Lunar Reconnaissance Orbiter (LRO) Narrow Angle Camera (NAC) imagery captured at $1\text{m}/\text{pixel}$ ground resolution. The trained neural network is applied to every rectangular image patch in the test image. In order to reduce the memory consumption, detection is ran on image blocks of 600×400 pixels The test patterns used by our system range from 2×2 pixels to 120×120 pixels. Detection results for patterns smaller than 8×8 pixels remain unreliable for the current system. For a test patch of a given scale to become a crater candidate its crater detection score must be higher than the detection score for the other classes (shadow and flat region) and must be above a fixed threshold. The threshold value varies based on the patch size to be investigated. We found experimentally that the threshold for smaller patches must be lower than the threshold for larger patches. At each scale the crater candidates are clustered and overlapping candidates are removed. For each cluster of overlapping patterns, the pattern with the higher score is kept, and the remaining patterns are dismissed. The clustering procedure is then applied across scales to remove overlapping patterns at different scales. Often a region of interest is covered by multiple LRO-NAC images. Craters are detected for each of the LRO-NAC images separately, and when combining the results, the craters in the overlapping regions across multiple images determine multiple detection for each crater. The location of these craters may not be perfectly aligned. The clustering method as described above is applied to cluster and remove these multiple detections for each crater. When the DEM is available together with the imagery, the crater detection results are validated and aligned with the corresponding DEM region. During the alignment, our method constraints that the center of the crater corresponds to the lowest local elevation point in DEM . Figure 2 illustrates the crater detection result before and after alignment with the DEM. The method described above uses models trained from data captured under the same sun and camera orientation as the test image. The crater appearances changes dramatically with the illumination conditions and a training set captured in different conditions than the test set leads to low accuracy detection results.

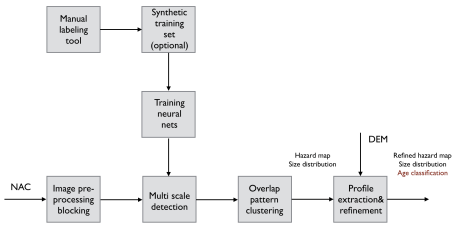

Figure 1: Overall crater detection system.

Alternatively, the training set can be derived by generating synthetic crater images from an existing high res-

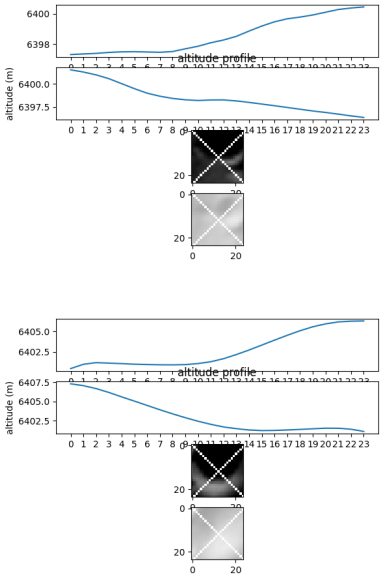

Figure 2: Elevation profiles, image and hillshade before (top) and after (bottom) alignment with the DEM.

olution DEM. The reflectance model R is given by

$$R_{ij} = (1 - L(\alpha)) \cos i + 2L(\alpha) \frac{\cos i}{\cos i + \cos e}. \quad (1)$$

where

$$L(\alpha) = 1 + A\alpha + B\alpha^2 + C\alpha^3. \quad (2)$$

and α is the phase angle measured in degrees, A, B, C a set of given coefficients, e and i are the emission and incidence angles respectively. For a set of craters labeled within an existing DEM, a set of synthetic crater images can be obtained using the Lunar reflectance model above and the camera pose and sun position at the time the test image was captured (Figure 3). This method allows to

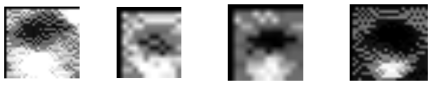

Figure 3: An example of synthetic craters derived from the Lunar DEM and the Lunar reflectance model.

re-use the labeled carter data and removes the need for recreating a training set for any test image captured under a new sun and camera orientation. The shadow and flat region sets can be re-used across images since their appearances varies more uniformly across images. Figure 4 compares the results of crater detection using the image and the synthetic training set. Figure 5 illustrates the result on the crater detection method on a typical LRO-NAC image sub region captured at the Lunar South Pole.

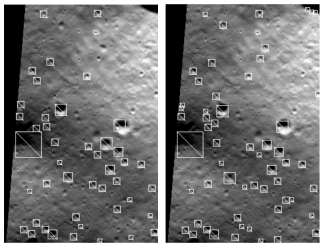

Figure 4: Crater detection results trained using image (left) and synthetic crater image (right) sets.

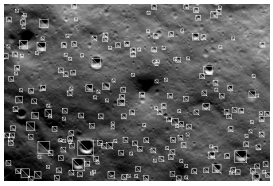

Figure 5: An example of synthetic craters derived from the Lunar DEM and the Lunar reflectance model.

References

[1] J. P. Cohen, H. Z. Lo, T. Lu, and W. Ding. Crater detection via convolutional neural networks. *arXiv preprint arXiv:1601.00978.*, 2016.

[2] E. Emami, Bebis, G., A. Nefian, and T Fong. Automatic crater detection using convex grouping and convolutional neural networks. *International Symposium on Visual Computing*, 2015.

[3] S. Ren and et al. Faster r-cnn: Towards real- time object detection with region proposal networks. *Advances in neural information processing systems*, 2015.

[4] E. Emami, Bebis G., A. Nefian, and T. Fong. On crater verification using mislocalized crater regions. *IEEE Winter Conference on Applications of Computer Vision*, 2017.